An Approach for the Qualitative Graphical Representation of the Describing Function in Nonlinear Systems Stability Analysis

Davide Tebaldi *Member, IEEE* and Roberto Zanasi

***Abstract*— The describing function method is a useful tool for the qualitative analysis of limit cycles in the stability analysis of nonlinear systems. This method is inherently approximate; therefore, it should be used for a fast qualitative analysis of the considered systems. However, plotting the exact describing function currently requires heavy mathematical calculations, reducing interest in this method. The objective of this paper is to enhance the standard describing function method by reducing the complexity of the calculations required to plot the describing function. To this end, a new method for the qualitative plotting of the describing function for piecewise nonlinearities involving discontinuities is proposed. This new method is presented in the form of an algorithm. However, unlike the standard method, which involves complex calculations for determining the describing function, the proposed approach also allows for a straightforward, hand-drawn plotting of the describing function using the rules introduced in this paper, simply by analyzing the shape of the nonlinearity. The proposed case studies show that the limit cycles estimation performed using the standard exact plotting of the describing function yields the same qualitative results as the proposed qualitative method for plotting the describing function.**

I. INTRODUCTION

Persistent oscillatory behaviors, typically referred to as limit cycles, are an inherent property of a large variety of systems of different nature, including biological [1], [2] and engineering [3]. Limit cycles are indeed present in engineering systems belonging to different energetic domains, including mechanical systems [4] such as robotic systems, electrical systems [5] such as electrical oscillators, and hydraulic systems [6] such as hydraulic actuators.

One of the most effective tools to study the existence and the characteristics of limit cycles is the describing function method [7]. With reference to the system of Fig. 1, limit cycles can exist under certain assumptions if the so-called self-sustaining equation $F(X)\,G(j\omega) = -1$ exhibits solutions, where $G(j\omega)$ is the frequency response function of the linear system $G(s)$, and $F(X)$ is the describing function of the considered nonlinearity. Despite being non-rigorous, the describing function method finds several applications, including photovoltaic systems [8], disturbance rejection in nonlinear active disturbance rejection control

The work was partly supported by the University of Modena and Reggio Emilia through the action FARD (Finanziamento Ateneo Ricerca Dipartimentale) 2023/2024, and funded under the National Recovery and Resilience Plan (NRRP), Mission 04 Component 2 Investment 1.5 - NextGenerationEU, Call for tender n. 3277 dated 30/12/2021 Award Number: 0001052 dated 23/06/2022.

The authors are with the Department of Engineering "Enzo Ferrari", University of Modena and Reggio Emilia, Modena, Via Pietro Vivarelli 10, 41125 Modena, Italy. E-mails: {davide.tebaldi, roberto.zanasi}@unimore.it.

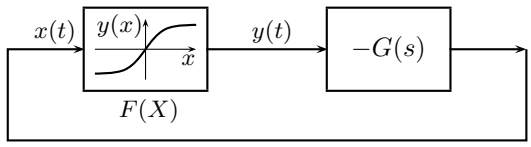

Fig. 1. Considered nonlinear autonomous feedback system.

[9], and the identification of the structural nonlinearities in a multi-degree-of-freedom nonlinear systems [10].

Through the years, many different modifications or additions to the describing function method have been made. In [11], a stability criterion is provided, giving an interesting justification of the quasi-static stability criterion upon which the describing function method is based. The describing function method is studied in [12] for limit cycles analysis in switched circuits, while a refinement of the approximated solution given by this method is proposed in [13] and an extension to systems exhibiting more than one nonlinearity in given in [14]. Thanks to computer aided control system design software, interactive tools have been developed for limit cycles analysis using the describing function method [15].

However, the use of graphical tools such as the fast hand-drawing of the describing function can be an important ability for control engineers. Indeed, despite being an effective method, the main limitation associated with the describing function is the derivation of the analytical expression of the describing function, which often requires a detailed analysis of the considered nonlinearity and is derived using heavy mathematical calculations [16]. Considering that the describing function method is non-rigorous since it is based on an approximated analysis [17], the complexity of calculation diminishes the easiness and interest of application of this method. The objective of this paper is therefore to enhance the standard describing function method by reducing the complexity of calculations to plot the describing function.

The main contributions of this paper are the following. 1) The proposal of an algorithm for the automatic plotting of the exact describing function of piecewise nonlinearities involving discontinuities. 2) The proposal of a new method for the qualitative plotting of the describing function for piecewise nonlinearities involving discontinuities. The proposed method consists in a series of rules for drawing the qualitative describing function by hand very quickly, by simply looking at the nonlinear characteristic. Furthermore, the proposed method is also translated in an algorithm involving simpler calculations than the standard complex analytical expression of the describing function $F(X)$. 3) The introduction of case studies showing that the analysis

and limit cycles estimation carried out using the qualitative describing function plotting give, qualitatively, the same results as using the standard describing function plotting. Furthermore, a property to determine the positioning of the limit cycles in the state space is also introduced.

The remainder of this paper is structured as follows. The describing function of two standard nonlinearities are reported in Sec. II, while the algorithm for plotting the describing function of piecewise nonlinearities with discontinuities is given in Sec. III. The new approach for the qualitative plotting of the describing function is proposed in Sec. IV, and applied to the limit cycle estimation of two case studies in Sec. V. The conclusions are given in Sec. VI.

II. Describing function

Let $x(t) = X\,\sin(\omega t)$ be the sinusoidal input of the nonlinear function $y(x)$ shown in Fig. 1. The corresponding output signal $y(t)$ is a periodic signal that can be expanded in a Fourier series as follows:

$$y(t) = \sum_{n=1}^{\infty} Y_n\,\sin\left(n\omega t + \varphi_n\right). \tag{1}$$

The constant term Y_0 is missing in (1) due to Assumption 1.

Assumption 1: Reference is made to the nonlinear feedback structure shown in Fig. 1, where the nonlinear function $y(x)$ is purely algebraic, symmetric with respect to the origin, i.e. $y(-x) = -y(x)$, and independent of the frequency ω of the input signal $x(t)$.

The use of the describing function is based on the following approximation: all the higher order harmonics (i.e. for $n \geq 2$) in the Fourier series (1) are neglected, while the first harmonic $y(t) \simeq Y_1(X)\ \sin\left(\omega t + \varphi_1(X)\right)$ is considered.

The describing function $F(X)$ of the nonlinear function $y(x)$ links the sinusoidal input $x(t) = X\,\sin(\omega t)$ to the first harmonic $Y_1(X)\ \sin\left(\omega t + \varphi_1(X)\right)$ of the output signal $y(t)$ [7] and, in the general case, is defined as follows:

$$F(X) = \frac{Y_1(X)}{X}\ e^{j\varphi_1(X)}, \tag{2}$$

where $Y_1(X) = \sqrt{a_1^2(X) + b_1^2(X)}$, $\varphi_1(X) = \arctan\,\frac{a_1(X)}{b_1(X)}$,

$$\begin{aligned} a_1(X) &= \tfrac{1}{\pi}\textstyle\int_{-\pi}^{\pi} y(X\sin\theta)\,\cos\theta\,d\theta, \\ b_1(X) &= \tfrac{1}{\pi}\textstyle\int_{-\pi}^{\pi} y(X\sin\theta)\,\sin\theta\,d\theta, \end{aligned} \tag{3}$$

and $\theta = \omega t$. Due to the symmetry hypothesis in Assumption 1, the coefficient $a_1(X)$ in (3) is zero, and the describing function $F(X)$ simplifies as follows [7]:

$$F(X) = \frac{b_1(X)}{X} = \frac{4}{\pi\,X}\int_0^{\frac{\pi}{2}} y(X\sin\theta)\,\sin\theta\,d\theta. \tag{4}$$

1) Dead Zone: The describing function $F_d(m, X_1, X)$ of the dead zone $y_d(x) = y_d(m_1, X_1, x)$ shown in Fig. 2(a) is the following [16]:

$$F_d(X) = F_d(m, X_1, X) = \begin{cases} 0 & \text{if} \quad X < X_1, \\ m\,\Phi\left(\frac{X}{X_1}\right) & \text{if} \quad X \geq X_1, \end{cases} \tag{5}$$

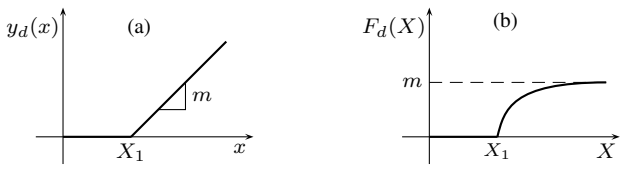

Fig. 2. (a) Dead zone function $y_d(x)$; (b) Describing function $F_d(X)$.

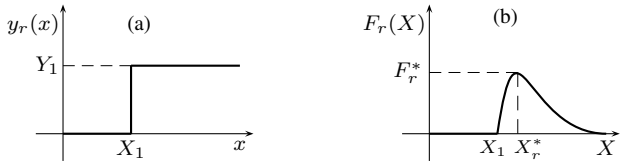

Fig. 3. (a) Relay with threshold $y_r(x)$; (b) Describing function $F_r(X)$.

where:

$$\Phi\left(\tfrac{X}{X_1}\right) = 1 - \tfrac{2}{\pi}\left(\arcsin\tfrac{X_1}{X} + \tfrac{X_1}{X}\sqrt{1-\left(\tfrac{X_1}{X}\right)^2}\right). \tag{6}$$

The shape of function $F_d(X)$ in (5) is shown in Fig. 2(b). The derivative of function $F_d(X)$ with respect to X is the following:

$$\frac{F_d(X)}{dX} = \frac{4mX_1(X^2 - X_1^2)}{\pi X^3\sqrt{X^2 - X_1^2}},$$

from which it follows that the slope of function $F_d(X)$ is zero for $X = X_1$ and is positive for $X > X_1$. This means that function $F_d(X)$ always increases for $X > X_1$ and reaches its maximum value m when $X \to \infty$.

2) Relay with threshold: The describing function $F_r(Y_1, X_1, X)$ of the relay with threshold $y_r(x) = y_r(Y_1, X_1, x)$ shown in Fig. 3(a) is [16]:

$$F_r(X) = F_r(Y_1, X_1, X) = \begin{cases} 0 & \text{if } X < X_1, \\ Y_1\,\Psi(X_1, X) & \text{if } X \geq X_1, \end{cases} \tag{7}$$

where:

$$\Psi(X_1, X) = \tfrac{4}{\pi X}\sqrt{1-\left(\tfrac{X_1}{X}\right)^2}. \tag{8}$$

The shape of function $F_r(X)$ is shown in Fig. 3(b). The derivative of function $F_r(X)$ with respect to X is:

$$\frac{F_r(X)}{dX} = \frac{4Y_1(2X_1^2 - X^2)}{\pi X^3\sqrt{X^2 - X_1^2}},$$

from which it follows that the slope of function $F_r(X)$ is infinite for $X = X_1$. The maximum F_r^* of function $F_r(X)$ occurs at $X = X_r^* = \sqrt{2}X_1$ and is given by $F_r^* = \frac{2Y_1}{\pi X_1}$.

III. Describing function $F(X)$ of piecewise nonlinear functions $y(x)$

The describing functions of several classes of specific nonlinearities have been determined [16]. In this paper, we focus on the computation of the describing function $F(X)$ of a *generic* piecewise nonlinear function $y(x)$.

Property 1: The describing function $F(X)$ of a piecewise nonlinear function $y(x)$ with discontinuities can always be obtained as a linear combination of a certain number of describing functions $F_d(X)$ and $F_r(X)$ of the two nonlinear functions $y_d(x)$ and $y_r(x)$ shown in Fig. 2 and Fig. 3.

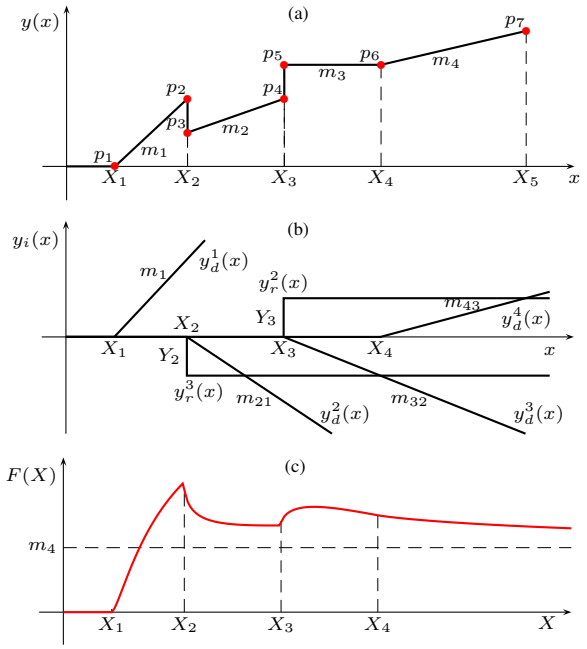

Fig. 4. (a) Piecewise nonlinear function $y(x)$; (b) Components of $y(x)$ in (9); (c) Describing function $F(X)$ in (10) computed using Algorithm 1.

Proof. Reference is made to the case study of Fig. 4(a). In this case, the function $y(x)$ can be obtained as the sum of six functions of type $y_d(x)$ and $y_r(x)$, as in Fig. 4(b):

$$\begin{aligned} y(x) = {} & y_d^1(m_1, X_1, x) + y_d^2(m_{21}, X_2, x) + y_r^2(Y_2, X_2, x) \\ & + y_d^3(m_{32}, X_3, x) + y_r^3(Y_3, X_3, x) + y_d^4(m_{43}, X_4, x) \,, \end{aligned} \tag{9}$$

where $m_{21} = m_2 - m_1$, $m_{32} = m_3 - m_2 = -m_2$ and $m_{43} = m_4 - m_3 = m_4$. From (9), it follows that the corresponding describing function $F(X)$, shown in Fig. 4(c), is the sum of six describing functions of type $F_d(X)$ and $F_r(X)$:

$$\begin{aligned} F(X) = {} & F_d(m_1, X_1, X) + F_d(m_{21}, X_2, X) + F_r(Y_1, X_2, X) \\ & + F_d(m_{32}, X_3, X) + F_r(Y_3, X_3, X) + F_d(m_{43}, X_4, X) \,. \end{aligned} \tag{10}$$

This decomposition can be done for any type of generic piecewise nonlinear function $y(x)$ with discontinuities. □

An algorithm for computing the describing function $F(X)$ of a piecewise nonlinear function $y(x)$ with discontinuities is reported in Algorithm 1. Let $p_i = (x_i, y_i)$, for $i \in \{1, 2, \ldots, r\}$, denote the points where function $y(x)$ changes its slope or has a discontinuity. The algorithm takes as input vectors $\mathbf{x} = [x_1, x_2, \ldots, x_r]$ and $\mathbf{y} = [y_1, y_2, \ldots, y_r]$, defining the position of points p_i, and vector $\mathbf{X} = (0 : \delta_X : X_m)$, containing the desired values of amplitude X of the input sinusoidal signal. The algorithm produces as output a vector $\mathbf{F}(\mathbf{X})$ containing the samples of the resulting describing function $F(X)$ in correspondence of the points in the input vector $\mathbf{X}$. The Matlab code of Algorithm 1 is freely available in the repository [18].

The points p_i corresponding to vectors $\mathbf{x} = [2, 5, 5, 9, 9, 13, 19]$ and $\mathbf{y} = [0, 4, 2, 4, 6, 6, 8]$ used for the example of Fig. 4 are highlighted in red in Fig. 4(a), while the describing function $F(X)$ given by Algorithm 1 is shown in Fig. 4(c).

Algorithm 1 Describing Function $\mathbf{F}(\mathbf{X})$

Input: $\mathbf{x}, \mathbf{y}, \mathbf{X}$
Output: $\mathbf{F}(\mathbf{X})$

```
Initialize F(X) = (0, 0, ..., 0) ∈ R^n, where n = dim(X);
Initialize i = 2;
while i < dim(x) do
    Find set S = (k, k+1, ..., n) s.t. X_k > x_i;
    if x_i = x_{i+1} then
        Compute discontinuity Y_k = y_{i+1} − y_i as in Fig. 3(a);
        Compute Ψ(x_i, X(S)) as in (8);
        Compute F(X) = F(X) + Y_k Ψ(x_i, X(S)) as in (7);
        Remove x_i from x; Remove y_i from y;
    end if
    Compute the two slopes m_i and m_{i+1} of the two segments
    [(x_{i−1}, y_{i−1}), (x_i, y_i)] and [(x_i, y_i), (x_{i+1}, y_{i+1})];
    Compute Φ(X(S)/x_i) as in (6);
    Compute F(X) = F(X) + (m_{i+1} − m_i) Φ(X(S)/x_i) as in (5);
    Increment index i = i + 1;
end while
return F(X)
```

IV. Describing Function $F(X)$: Qualitative Graphical Representation

Despite the describing function method being non-rigorous, the exact calculation of the describing function $F(X)$ usually requires complex analytical calculations. This numerical complexity greatly limits the use of this method. In this section, an intuitive and fast approach for the qualitative graphical representation of function $F(X)$ is proposed.

Property 2: Qualitative graphical behavior $\tilde{F}(X)$ of function $F(X)$. Let $y(x)$ be a nonlinear function with discontinuities, let X_j, for $j \in \{1, 2, \ldots, r\}$, be the values of x where function $y(x)$ has a discontinuity or changes its slope from m_{j-1} to m_j, let vectors $\overline{\mathbf{X}}$ and $\mathbf{m}$ be defined as follows $\overline{\mathbf{X}} = [0, X_1, \ldots, X_r]$ and $\mathbf{m} = [m_0, m_1, \ldots, m_r]$, let $\overline{\mathbf{X}}_d \in \overline{\mathbf{X}}$ be a subset of vector $\overline{\mathbf{X}}$ containing all the values X_j where function $y(x)$ has a discontinuity, and let $\overline{\mathbf{Y}}_d$ be the vector of all the discontinuity amplitudes Y_j that occur at $X = X_j \in \overline{\mathbf{X}}_d$. The qualitative graphical behavior $\tilde{F}(X)$ of function $F(X)$ can be determined using the following rules:

1) Function $\tilde{F}(X)$ is always continuous for $X > 0$.

2) If function $y(x)$ is discontinuous for $x = 0$, then the initial value of function $\tilde{F}(X)$ is infinite: $\tilde{F}(X)|_{X=0} = \infty$.

3) For $X \leq X_1$, the value of function $\tilde{F}(X)$ is equal to the slope m_0 of the first segment of function $y(x)$.

4) For $X \to \infty$, the value of function $\tilde{F}(X)$ is equal to the slope m_r of the last linear segment of function $y(x)$.

5) Let $\tilde{F}_j(X)$ denote the qualitative graphical behavior of function $F(X)$ within the range $X \in [X_j, X_{j+1}]$ where function $y(x)$ has slope m_j. The sequence of qualitative functions $\tilde{F}_j(X)$, for $j \in \{0, 1, \ldots, r\}$, can be plotted using Algorithm 2, where: a) $\tilde{\Phi}\left(\frac{X}{X_j}\right)$ is an exponential-like function, having a shape similar to that of function $F_d(X)$ shown in Fig. 2(b): it is equal to zero until $X = X_j$, where it has null slope, and then tends to one when $X \to \infty$; b) $\tilde{\Psi}(X, X_j)$ is an impulsive function, having a shape similar

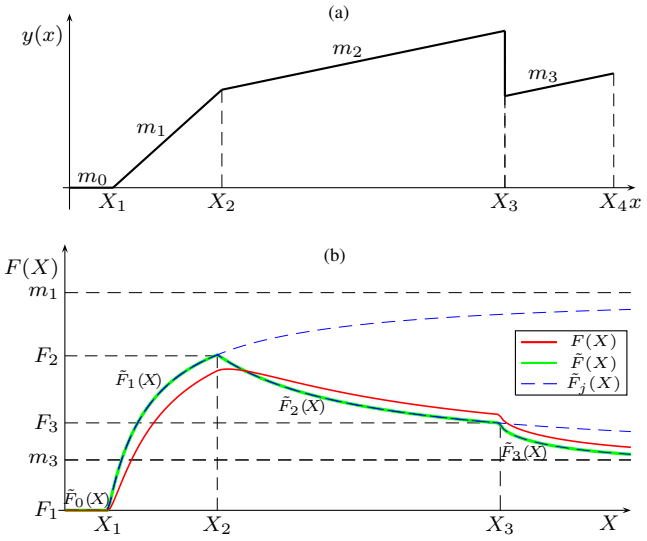

Fig. 5. (a) Piecewise nonlinear function $y(x)$. (b) Describing function $F(X)$ of function $y(x)$, corresponding qualitative graphical representation $\tilde{F}(X)$, and exponential-like function $\tilde{F}_j(X)$ for $j \in \{0,\ 1,\ 2,\ 3\}$.

to that of function $F_r(X)$ shown in Fig. 3(b): it is equal to zero until $X = X_j$, where it has infinite slope, reaches its maximum $\frac{2}{\pi X_j}$ for $X = \sqrt{2}X_j$, and then tends to zero when $X \to \infty$. The value of the first function $\tilde{F}_0(X)$, for $X \in [0,\ X_1]$, is equal to the first slope m_0 of function $y(x)$. The qualitative function $\tilde{F}_j(X)$, for $j \in \{1, 2, \ldots, r\}$, starts from the value $\tilde{F}_{j-1}(X_j)$ and then tends to the value m_j for $X \to \infty$. If a discontinuity occurs at $X = X_j$, then an additional term $Y_j\tilde{\Psi}(X, X_j)$ must be added to function $\tilde{F}_j(X)$. The obtained function $\tilde{F}_j(X)$ must be considered only within the range $X \in [X_j,\ X_{j+1}]$. The value $\tilde{F}_j(X_{j+1})$ is then used as starting point for plotting the qualitative function $\tilde{F}_{j+1}(X)$ in the next range $X \in [X_{j+1}, X_{j+2}]$. □

Qualitative proofs of the aforementioned rules:

1) Function $\tilde{F}(X)$ is always continuous because the describing functions $F_d(X)$ and $F_r(X)$, composing function $F(X)$, are continuous, see Prop. 1, Fig. 2 and Fig. 3.

2) If $y(x)$ is discontinuous for $x = 0$, then $\tilde{F}(X)|_{X=0} = \infty$ because, when $X \to 0$, the amplitude $Y_1(X)$ in (2) of the first harmonic of signal $y(t)$ is finite: $Y_1(X) = \frac{4Y_1}{\pi}$.

3) For $X \leq X_1$, function $y(x)$ is linear, the output signal $y(t) = m_0\, x(t)$ is proportional to $x(t)$, and $\tilde{F}(X) = m_0$ because the ratio $Y_1(X)/X$ in (2) is equal to the slope m_0.

4) When $X \to \infty$, the slope m_r of the last segment of function $y(x)$ becomes increasingly important for the shape of the output signal $y(t)$: when $X \to \infty$, $y(t) \simeq m_r x(t)$ and, therefore, $\tilde{F}(X)|_{X\to\infty} = m_r$.

5) Reference is made to the nonlinear function $y(x)$ shown in Fig. 5(a), defined by vectors $\mathbf{x} = [2, 7, 20, 20, 25]$ and $\mathbf{y} = [0, 4.5, 7.21, 4.21, 5.25]$. The corresponding describing function $F(X)$ (red solid line) and qualitative graphical representation $\tilde{F}(X)$ (green solid line) are shown in Fig. 5(b). The steps for plotting the qualitative function $\tilde{F}(X)$ are: a) For $X \leq X_1$, the qualitative function is $\tilde{F}_0(X) = 0$, because the slope of the first segment of function $y(x)$ is zero. b) Within the range $X \in [X_1,\ X_2]$, a correct qualitative description of function $F(X)$ is described by the exponential-like function $\tilde{F}_1(X)$ starting from point $(X_1, 0)$ and reaching the value m_1 for $X \to \infty$, see the blue dashed line in Fig. 5(b). c) Within the range $X \in [X_2,\ X_3]$, function $F(X)$ is qualitatively described by function $\tilde{F}_2(X)$, starting from point $(X_2, \tilde{F}_1(X_2))$ and reaching value $m_2 = m_3$ for $X \to \infty$. d) For $X > X_3$, function $F(X)$ is qualitatively described by function $\tilde{F}_3(X)$, starting from point $(X_3, \tilde{F}_2(X_3))$ and reaching value $m_2 = m_3$ for $X \to \infty$.

Algorithm 2 Qualitative Function $\tilde{\mathbf{F}}(\mathbf{X})$

Input: $\mathbf{X}$, $\overline{\mathbf{X}}$, $\mathbf{m}$, $\overline{\mathbf{X}}_d$, $\overline{\mathbf{Y}}_d$
Output: $\tilde{\mathbf{F}}(X)$

```
Find set S_0 = (0, 1, ..., n) s.t. X(S_0)) ≤ X_1;
Compute F̃_0(X(S_0)) = m_0;
Compute F̃(X(S_0)) = F̃_0(X(S_0));
for j ← 1 to dim(X̄) do
    Find set S = (k, k+1, ..., k+n) s.t. X_j < X(S)) ≤ X_{j+1};
    Compute F̃_{j0} = F̃_{j-1}(X_j);
    Compute F̃_j(X(S)) = F̃_{j0} + (m_j − F̃_{j0}) Φ̃(X(S)/X_j);
    if X_j ∈ X̄_d then
        Compute F̃_j(X(S)) = F̃_j(X(S)) + Y_j Ψ̃(X(S), X_j);
    end if
    Compute F̃(X(S)) = F̃_j(X(S));
end for
return F̃(X)
```

Remark 1: When applying the describing function method, it is an interesting and useful feature to firstly discriminate whether stable/unstable persistent oscillations - known as limit cycles - are present in the system in a fast way, before delving into the calculations to determine their amplitude and frequency. While the standard describing function method does not allow for such initial fast analysis, the new proposed approach for plotting the so-called *qualitative describing function* does. In fact, while the qualitative function $\tilde{F}(X)$ in Fig. 5(b) was plotted using Algorithm 2 with $\tilde{\Phi}\left(\frac{X}{X_j}\right) = 1 - \frac{X}{X_j}$ and $\tilde{\Psi}(X, X_j) = \Psi(X, X_j)$, a different but qualitatively similar plot can also be effectively drawn by hand by directly applying steps from 1) to 5) in Sec. IV. Furthermore, the qualitative describing function $\tilde{F}(X)$ captures the behavior of the actual describing function $F(X)$ with no need to perform the complex calculations in (5), (8) and (10). Therefore, a simple hand-drawn sketch of the qualitative describing function $\tilde{F}(X)$ is sufficient to identify stable/unstable limit cycles in the system with sufficient detail, as discussed in the next section.

V. Describing Function: Limit Cycles Estimation

An estimation of the limit cycles present in the nonlinear feedback system of Fig. 1 can be performed by using the following complex self-sustaining equation: $F(X)\,G(j\omega) = -1$. This nonlinear equation is generally solved graphically by plotting both the functions $G(j\omega)$ and $-1/F(X)$ on the complex plane [7]. The intersection points $P_i(\omega_i, X_i)$ between $G(j\omega)$ and $-1/F(X)$ provide a good estimation of the frequencies ω_i and the amplitudes X_i of the limit cycles.

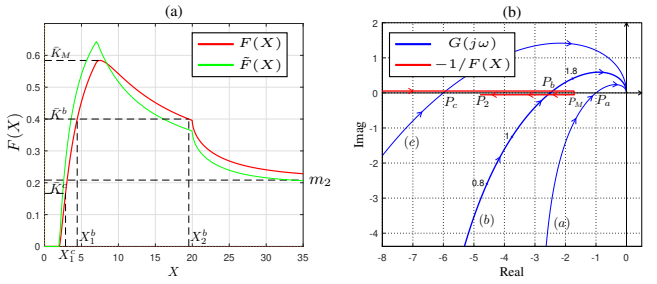

Fig. 6. Case study of Sec. V-A. (a) Qualitative and actual describing functions $F(X)$ and $\tilde{F}(X)$ of the nonlinear function $y(x)$ in Fig. 5(a). (b) Graphical solution of equation $F(X)\,G(j\omega) = -1$ on the Nyquist plane.

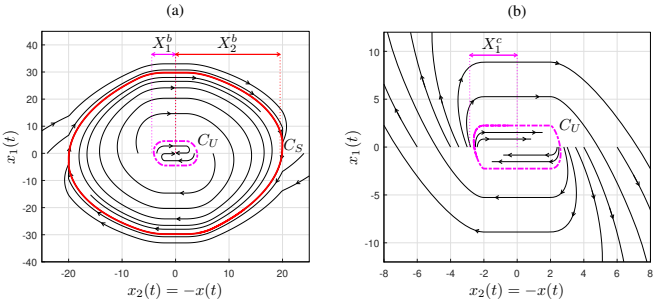

Fig. 7. Case study of Sec. V-A. (a) State space trajectories in case (b) of Fig. 6(b); the stable limit cycle C_S (red closed line) is defined by point $P_{b2} = (\bar{\omega}, X_2^b)$, and the unstable limit cycle C_U (magenta dashed closed line) is defined by point $P_{b1} = (\bar{\omega}, X_1^b)$. (b) State space trajectories in case (c) of Fig. 6(b); the unstable limit cycle C_U (magenta dashed closed line) is defined by point $P_c = (\bar{\omega}, X_1^c)$.

Due to Assumption 1, all the nonlinear functions $y(x)$ considered in this work are characterized by a positive real describing function $F(X)$, and therefore all the intersection points $P_i(\omega_i, X_i)$ are on the negative real semiaxis. Furthermore, it is well known that [7]: 1) an intersection point $P_i(\omega_i, X_i)$ corresponds to a stable limit cycle if, for increasing X, the point $-1/F(X)$ exits from the Nyquist diagram of function $G(j\omega)$, and to an unstable limit cycle in the opposite case. 2) the frequency and amplitude ω_i and X_i of the limit cycle correspond to the frequency where function $G(j\omega_i)$ intersects the real negative semiaxis and to the value X_i such that $F(X_i) = \bar{K}$, respectively, where $\bar{K}$ is the gain margin of the transfer function $G(s)$.

The limit cycle generated by signal $y(t)$ in the state space of system $G(s)$ can be approximately determined as follows. Let $\mathcal{S} = (\mathbf{A}, \mathbf{B}, \mathbf{C}, \mathbf{D})$ be a state space realization of the transfer function $G(s)$. The Laplace transform $\mathbf{X}(s)$ of state space vector $\mathbf{x}(t)$ of $\mathcal{S}$ can be expressed as follows:

$$\mathbf{X}(s) = \mathbf{H}(s)\,Y(s), \qquad \mathbf{H}(s) = (s\,\mathbf{I} - \mathbf{A})^{-1}\mathbf{B}, \tag{11}$$

where $Y(s)$ is the Laplace transform of the input $y(t)$. If only the first harmonic $y(t) = y_1(t) = Y_1 \sin(\omega t + \varphi_1)$ is considered, the steady-state vector $\tilde{\mathbf{x}}(t)$ at steady-state is:

$$\tilde{\mathbf{x}}(t) = \lim_{t\to\infty} \mathbf{x}(t) = \mathbf{A}(\omega)\sin(\omega t + \boldsymbol{\varphi}(\omega)). \tag{12}$$

where $\mathbf{A}(\omega) = Y_1\,|\mathbf{H}(j\omega)|$ and $\boldsymbol{\varphi}(\omega) = \arg(\mathbf{H}(j\omega)) + \varphi_1$.

Property 3: The steady-state vector $\tilde{\mathbf{x}}(t)$ in (12) belongs to the 2-dimensional subspace $\mathcal{X}_\omega = \text{span}\left(\tilde{\mathbf{x}}(0), \tilde{\mathbf{x}}(\frac{\pi}{2\omega})\right)$, where $\tilde{\mathbf{x}}(0) = \tilde{\mathbf{x}}(t)|_{t=0}$ and $\tilde{\mathbf{x}}(\frac{\pi}{2\omega}) = \tilde{\mathbf{x}}(t)|_{t=\frac{\pi}{2\omega}}$.

Proof. From (12), vector $\tilde{\mathbf{x}}(t)$ can be expressed as follows:

$$\tilde{\mathbf{x}}(t) = \sin(\omega t)\underbrace{\mathbf{A}(\omega)\sin\boldsymbol{\varphi}(\omega)}_{\tilde{\mathbf{x}}(0)} + \cos(\omega t)\underbrace{\mathbf{A}(\omega)\cos\boldsymbol{\varphi}(\omega)}_{\tilde{\mathbf{x}}(\frac{\pi}{2\omega})}$$

that is, for $t > 0$, vector $\tilde{\mathbf{x}}(t)$ can be expressed as a linear combination of the two vectors $\tilde{\mathbf{x}}(0)$ and $\tilde{\mathbf{x}}(\frac{\pi}{2\omega})$. □

A. First Case Study

Reference is made to the feedback system of Fig. 1, where $G(s) = \frac{k\,(2-s)}{s(s+1)}$ and $y(x)$ is the nonlinear function defined in Fig. 5(a). The Nyquist diagrams of function $G(s)$ for $k = 1$, $k = 2.5$ and $k = 6$ are shown in Fig. 6(b), see labels (a), (b) and (c), respectively. The intersection points of function $G(s)$ with the negative real semiaxis are denoted by $P_a = -\frac{1}{\bar{K}^a}$, $P_b = -\frac{1}{\bar{K}^b}$ and $P_c = -\frac{1}{\bar{K}^c}$, and are characterized by the same frequency $\bar{\omega} = \sqrt{2}$ and by the gain margins $\bar{K}^a = 1$, $\bar{K}^b = 0.4$ and $\bar{K}^c = 0.166$. The actual and qualitative describing functions $F(X)$ and $\tilde{F}(X)$ are shown in Fig. 6(a). The points P_2 and P_M in Fig. 6(b) are defined as follows: $P_2 = -\frac{1}{m_2}$ and $P_M = -\frac{1}{\bar{K}_M}$. The points P_a, P_c and P_c correspond to the following three working conditions: a) $\bar{K}^a > \bar{K}_M$: function $-\frac{1}{F(X)}$ is outside the Nyquist diagram of function $G(j\omega)$, therefore the origin of the feedback system is globally asymptotically stable. b) $\bar{K}_M > \bar{K}^b > m_2$: function $-\frac{1}{F(X)}$ intersects $G(j\omega)$ in two points: $P_{b1} = (\bar{\omega}, X_1^b)$ and $P_{b2} = (\bar{\omega}, X_2^b)$. The state space trajectories in the vicinity of the origin are shown Fig. 7(a), where $x(t) = -x_2(t)$ is the output of system $G(s)$. The simulated amplitudes X_1^b and X_2^b of Fig. 7(a) are quite similar to the amplitudes X_1^b and X_2^b in the analysis of Fig. 6(a) when $F(X) = \bar{K}^b$. c) $\bar{K}^c < m_2$: function $-\frac{1}{F(X)}$ intersects $G(j\omega)$ in point $P_c = (\bar{\omega}, X_1^c)$, corresponding to the unstable limit cycle C_U of Fig. 7(b): depending on the initial condition (y_0, x_0), the system trajectories either tend to the origin or to infinity.

Note that the actual and qualitative describing functions $F(X)$ and $\tilde{F}(X)$ in Fig. 6(a) are qualitatively similar, thus the same conclusions as the aforementioned analysis in terms of existence of stable/unstable limit cycles in the feedback system can be achieved using the proposed hand-drawn sketch of the qualitative describing $\tilde{F}(X)$ as in Remark 1.

B. Second Case Study

Let us consider the feedback system in Fig. 1 where $G(s) = \frac{k}{s(s+1)(s+3)}$ and $y(x)$ is the nonlinear function defined in Fig. 8(a). The Nyquist diagrams of function $G(s)$ for $k = 5$, $k = 15$ and $k = 30$ are shown in Fig. 9(b), see labels (a), (b) and (c), respectively. The intersection points $P_a = -\frac{1}{\bar{K}^a}$, $P_b = -\frac{1}{\bar{K}^b}$ and $P_c = -\frac{1}{\bar{K}^c}$ in Fig. 9(b) are characterized by the same frequency $\bar{\omega} = \sqrt{3}$ and gain margins $\bar{K}^a = 2.4$, $\bar{K}^b = 0.8$ and $\bar{K}^c = 0.4$. The actual and qualitative describing functions $F(X)$ and $\tilde{F}(X)$ are shown in Fig. 9(a). Three cases are considered: 1) Point P_a, which does not intersect function $-1/F(X)$, corresponds to the global asymptotic stability of the origin. 2) The intersection point P_c corresponds to the presence of a stable limit cycle, see Fig. 8(b): all the trajectories in the 3D space (black lines)

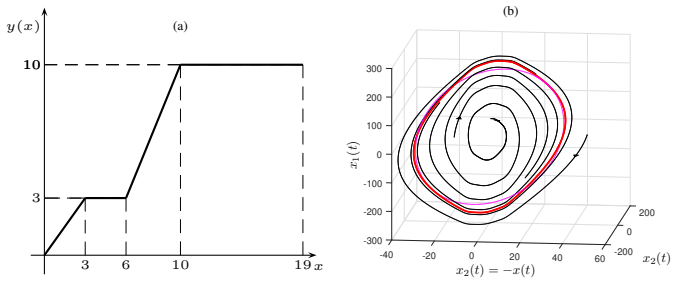

Fig. 8. Case study of Sec. V-B. (a) Nonlinear function $y(x)$. b) State space trajectories in case (c) of Fig. 9(b).

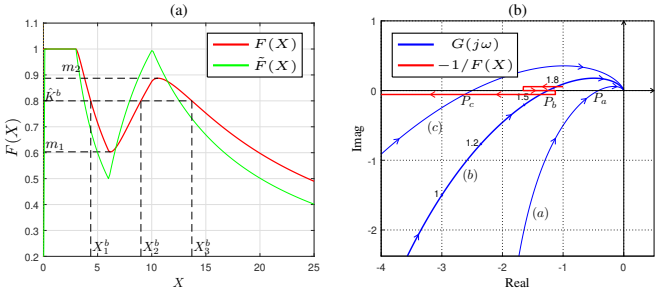

Fig. 9. Case study of Sec. V-B. (a) Qualitative and actual describing functions $F(X)$ and $\tilde{F}(X)$ of the nonlinear function $y(x)$ in Fig. 8(a). (b) Graphical solution of equation $F(X)\,G(j\omega) = -1$ on the Nyquist plane.

tend to the stable limit cycle (red line), and the magenta line denotes the limit cycle estimation $\tilde{\mathbf{x}}(t) \in \mathcal{X}_\omega$, defined in Prop. 3. 3) Point P_b, which intersects function $-1/F(X)$ three times, corresponds to the presence of three limit cycles, see Fig. 10: the two solid red lines denote the two stable limit cycles. The black and blue state space trajectories tend to the outer and inner stable limit cycles, respectively. The three magenta lines in Fig. 10 denote the three limit cycle estimations $\tilde{\mathbf{x}}_i(t) \in \mathcal{X}_\omega$ described in Prop. 3.

Even in this case, the actual and qualitative describing functions $F(X)$ and $\tilde{F}(X)$ in Fig. 9(a) are qualitatively similar, denoting that the same conclusions in terms of existence of stable/unstable limit cycles in the feedback system can be achieved using the proposed hand-drawn sketch of the qualitative function $\tilde{F}(X)$ as in Remark 1.

VI. Conclusions

This paper has introduced a new method for qualitatively plotting the describing function of piecewise nonlinearities involving discontinuities. The method is presented as an algorithm and, unlike the standard approach, which involves heavy calculations for the describing function computation, it effectively leads to a fast hand-drawing of the qualitative describing function by following the proposed rules, starting from the characteristics of the considered nonlinearity. The analysis of limit cycles in two numerical case studies has then been performed, showing that the same qualitative results can be obtained using the standard exact plotting and the proposed qualitative plotting of the describing function.

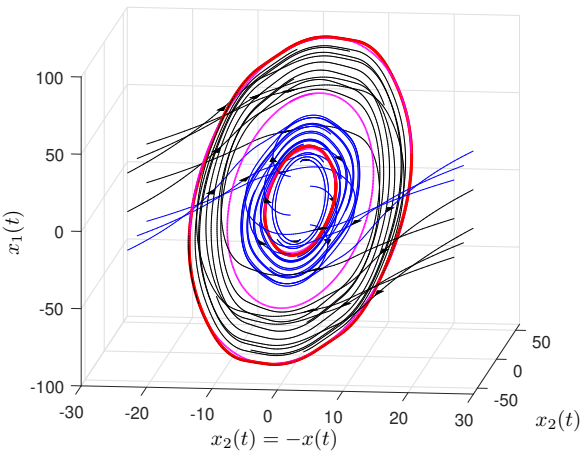

Fig. 10. Case study of Sec. V-B: state space trajectories in case (b) of Fig. 9(b).

References

[1] M. McCreesh, T. Menara, and J. Cortés, "Sufficient conditions for oscillations in competitive linear-threshold brain networks," *IEEE Control Systems Letters*, vol. 7, pp. 2886–2891, 2023.

[2] K. Kuritz, S. Zeng, and F. Allgöwer, "Ensemble controllability of cellular oscillators," *IEEE Control Syst. Lett.*, vol. 3, no. 2, pp. 296–301, 2019.

[3] J. Buchli, L. Righetti, and A. J. Ijspeert, "Engineering entrainment and adaptation in limit cycle systems," *Biol Cybern*, vol. 95, pp. 645–664, 2006.

[4] A. Reza Hakimi and T. Binazadeh, "Robust generation of limit cycles in nonlinear systems: Application on two mechanical systems," *J. Comput. Nonlinear Dyn.*, vol. 12, no. 4, p. 041013, 2017.

[5] V. Kyurkchiev and N. Kyurkchiev, "On an extended relaxation oscillator model: number of limit cycles, simulations. i," *Communications in Applied Analysis*, vol. 26, pp. 19–42, 2022.

[6] M. Ruderman, S. Kaltenbacher, and M. Horn, "Pressure-flow dynamics with semi-stable limit cycles in hydraulic cylinder circuits," in *2021 IEEE International Conference on Mechatronics (ICM)*, 2021, pp. 1–6.

[7] L. C. Goldfarb, "On some nonlinear phenomena in regulatory systems," *Frequency Response, R. Oldenburger, Ed., The Mac- millan Co., New York, N. Y*, pp. 239–259, 1956, this is an English translation of the original article which appeared in the Russian journal Avtomatika i Telemekhanika, vol. 8, pp. 349-383; Sept.-Octob., 1947.

[8] Q. Zhang, L. Zhou, M. Mao, B. Xie, and C. Zheng, "Power quality and stability analysis of large-scale grid-connected photovoltaic system considering non-linear effects," *IET Power Electronics*, vol. 11, no. 11, pp. 1739–1747, 2018.

[9] D. Wu and K. Chen, "Frequency-domain analysis of nonlinear active disturbance rejection control via the describing function method," *IEEE Trans. Ind. Electron.*, vol. 60, no. 9, pp. 3906–3914, 2013.

[10] Z. Zhao, C. Li, K. Ahlin, and H. Du, "Nonlinear system identification with the use of describing functions – a case study," *Vibroengineering PROCEDIA*, vol. 8, pp. 33–38, 2016.

[11] R. Miller, A. Michel, and G. Krenz, "On the stability of limit cycles in nonlinear feedback systems: Analysis using describing functions," *IEEE Trans. Circuits Syst.*, vol. 30, no. 9, pp. 684–696, 1983.

[12] S. Sanders, "On limit cycles and the describing function method in periodically switched circuits," *IEEE Trans. Circuits Syst. I, Fundam. Theory Appl.*, vol. 40, no. 9, pp. 564–572, 1993.

[13] I. Boiko, "Refinement of periodic solution obtained via describing function method," in *2006 American Control Conference*, 2006.

[14] J. Taylor, "Describing function method for limit cycle analysis of highly nonlinear systems," 08 1981.

[15] S. Dormido, C. Lampón, J. Díaz, and R. Costa-Castelló, "Describing function and event based analysis of a general class of piecewise feedback control systems," *IFAC-PapersOnLine*, vol. 58, no. 7, pp. 364–369, 2024, 4th IFAC Conference on Advances in Proportional-Integral-Derivate Control PID 2024.

[16] R. Sridhar, "A general method for deriving the describing functions for a certain class of nonlinearities," *IRE Transactions on Automatic Control*, vol. 5, no. 2, pp. 135–141, 1960.

[17] S. Engelberg, "Limitations of the describing function for limit cycle prediction," *IEEE Trans. Autom. Control.*, vol. 47, no. 11, pp. 1887–1890, 2002.

[18] D. Tebaldi and R. Zanasi, “Describing function plotting,” 2025, accessed: March 2025. [Online]. Available: https://it.mathworks.com/matlabcentral/fileexchange/180308-describing-function-plotting